Supplement

Table S1: AAOD for AeroCom Phase II using emission for year 2000. For details see Myhre et al. (2013).

Model	AAOD
BCC	0.0023
CAM4-Oslo	0.0047
CAM5.1	0.0069
GISS-MATRIX	0.0076
GISS-OMA	0.0055
GMI	0.0035
GOCART	0.0073
HadGEM2	0.0033
IMPACT-Umich	0.0032
INCA	0.0029
ECHAM5-HAM	0.0032
OsloCTM2	0.0043
SPRINTARS	0.0028
TM5	0.0020
Mean	**0.0042**
Median	**0.0034**
Std.dev	**0.0019**

Table S2: Refractive indices for BC, OA, and dust.

Model	BC refractive index (550 nm)	OA refractive index (550 nm)	Dust refractive index (550 nm)
CAM5-ATRAS	1.95 + 0.79 i	1.53 + 5.7E-3 i	1.51 + 2.1E-3 i
EC-Earth3	1.85 + 0.71 i	1.53 + 5.5E-3 i	1.52 + 1.1E-3 i
ECHAM-HAM	1.85 + 0.71 i	1.53 + 5.5E-3 i	1.45 + 1.0E-3 i
ECHAM-SALSA	1.85 + 0.71 i	1.53 + 5.5E-3 i	1.53 + 1.1E-3 i
ECMWF-IFS	1.75 + 0.45 i	1.53 + 0.015 i	1.53 + 5.2E-3 i
GEOS	1.75 + 0.45 i	1.53 + 5.0E-3 i	1.53 + 7.8E-3 i
GFDL-AM4	1.75 + 0.44 i	1.53 + 6.0E-3 i	1.49 + 2.0E-3 i
GISS-MATRIX	1.85 + 0.71 i	1.53 + 0.014i	1.56 + 2.2E-3 i
GISS-OMA	1.85 + 0.71 i	1.53 + 0.014 i	1.56 + 2.0E-3 i
INCA	1.75 + 0.44 i	1.53 + 5E-3 i	1.52 + 1.5E-3 i
NorESM2	1.95 + 0.79 i	1.53 + 6E-3 i	1.53 + 2.4E-3 i
OsloCTM3	1.75 + 0.44 i	1.53 + 0.033*	1.55 + 3.1E-3 i
SPRINTARS	1.75 + 0.44 i	1.53 + 6.0E-3 i	1.53 + 2.0E-3 i
TM5	1.85 + 0.71 i	1.53 + 5.5E-3 i	1.52 + 1.1E-3 i

Location	MAC [m^2 g^{-1}] (550)	MAC [m^2 g^{-1}] at reported wavelength	Reference
Large set of data	7.5 ± 1.2 and 11 m^2 g^{-1} at 550 nm for fresh and aged BC particles		Bond and Bergstrom (2006)
Urban	6.8 – 8.7		Hitzenberger et al. (2006)

Mexico City	8.7-8.9	5.5-5.6 (870)[1]	Doran et al. (2007)
Mexico	13.1	10.9 (660)	Subramanian et al. (2010)
High altitude (winter) High altitude (summer)	8.6 12.7	7.5 (630) 11 (630)	Cozic et al. (2008)
Denver	9.7	10 (532)[2]	Knox et al. (2009)
Different sites in India	7.4 – 17.3	Between 6 and 14 (at 678 nm)	Ram and Sarin (2009)
Urban (Barcelona) Traffic (Bern) Industrial (Huelva)	10.7 11.9 11.4	9.2 (637) 10.3 (637) 9.8 (637)	Reche et al. (2011)
Urban (Paris)	13.8	8.6 (880)	Laborde et al. (2013)
Shenzhen (China)	6.3	6.5 ± 0.5 (532)	Lan et al. (2013)
South Texas	7.8	8.1 (532)	Levy et al. (2013)
Mediterranean basin, remote, high-altitude site	12.6	10.9 ± 3.5 (637)	Pandolfi et al. (2014)
Arctic	5.7	around 6 (522 nm)	Yttri et al. (2014)
Pacific, the HIPPO campaign, pristine	11.3 (550)	11.3 (550)	Wang et al. (2014)
Rural North China	12.3	10 (678)	Cui et al. (2016)
Flare emission plumes in North Dakota	15.4 ± 11.5	16 ± 12 (530)	Weyant et al. (2016)
Lab measurements mimicking observations in Mexico city	7.89 ± 0.25	7.89 ± 0.25 (550)	You et al. (2016)
Aspvreten (SE) Birkenes (NO Finokalia (GR) Harwell (GB) Ispra (IT) Melpitz (DE) Montseny (ES) Puy de D^ome (FR) Vavihill (SE)	9.8 9.1 14.3 15.6 11.1 10.7 10.3 20.0 7.5	8.51 (637) 7.86 (637) 12.4 (637) 13.5 (637) 9.61 (637) 9.23 (637) 8.92 (637) 17.3 (637) 6.47(637)	Zanatta et al. (2016)
Urban China		14.6 ± 5.6 (532)	Wang et al. (2017)
Fresno, Italy	7.4	7.9 ± 1.5 (532)	Presler-Jur et al. (2017)
Urban North China Rural North China (mountain)	9.1 9.6	7.4 ± 2.6 7.8 ± 2.7	Bai et al. (2018)
Maldives	16.4	13.3 ± 4.2 (678)	Budhavant et al. (2020)
GoPoEx 2014 campaign, East Asia	6.6	6.4 ± 1.5 (565)	Cho et al. (2019)
Northwest China	13.3	8.3 (880) as an average of 7.4, 5.7, 8.1 and 12.1	Zhang et al. (2019)
Milan, Italy	9.9	10.2 (532)	Forello et al. (2019)
China	11.4	11.8 (532)	Ma et al. (2020)

Conversion formula, where we assume Ångstrøm exponent to be 1: MAC_atXnm*exp(-alog(550./X.))

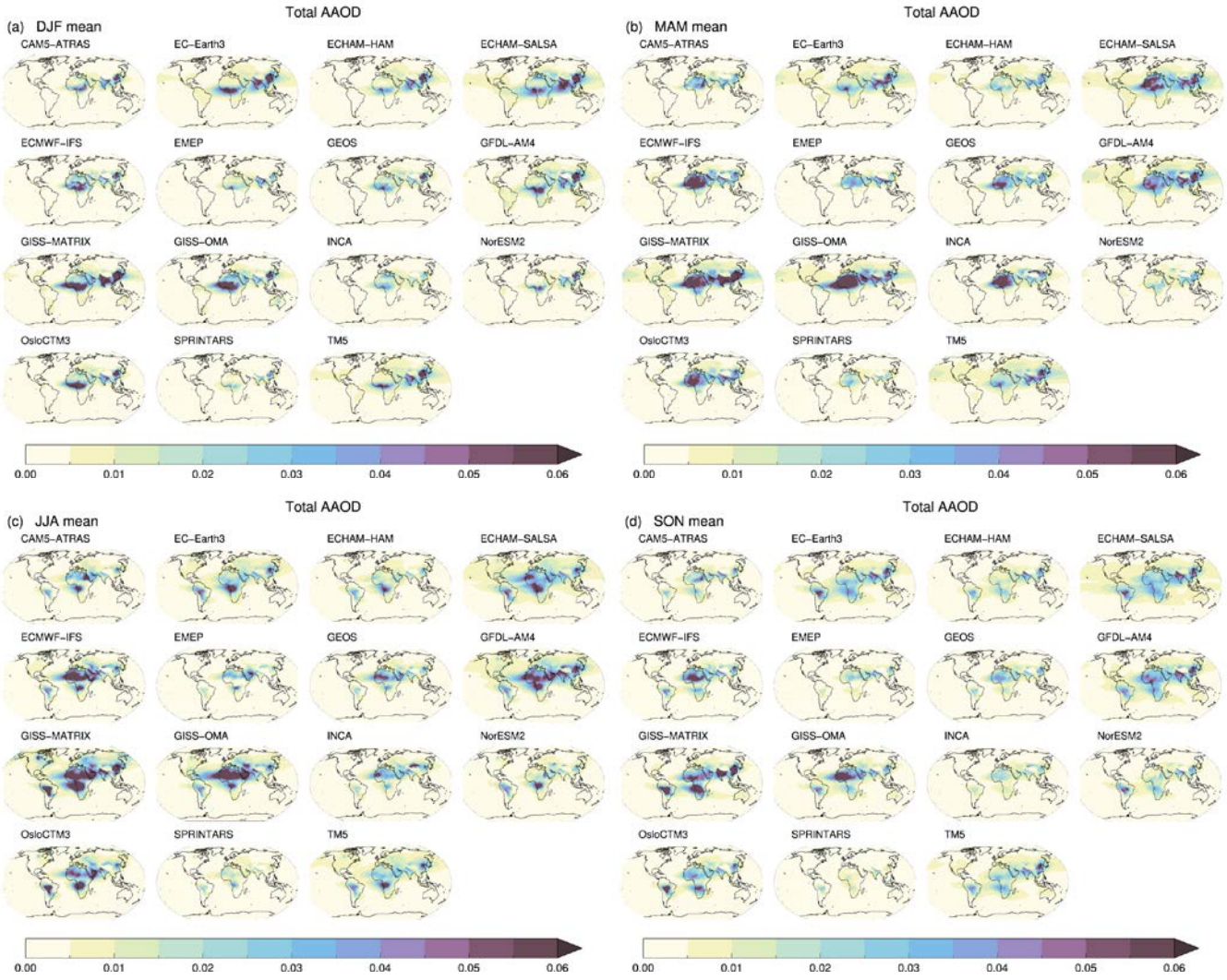

Figure S1: Total AAOD at λ = 550nm in AeroCom Phase III; (a) DJF mean, (b) MAM mean, (c) JJA mean, (d) SON mean

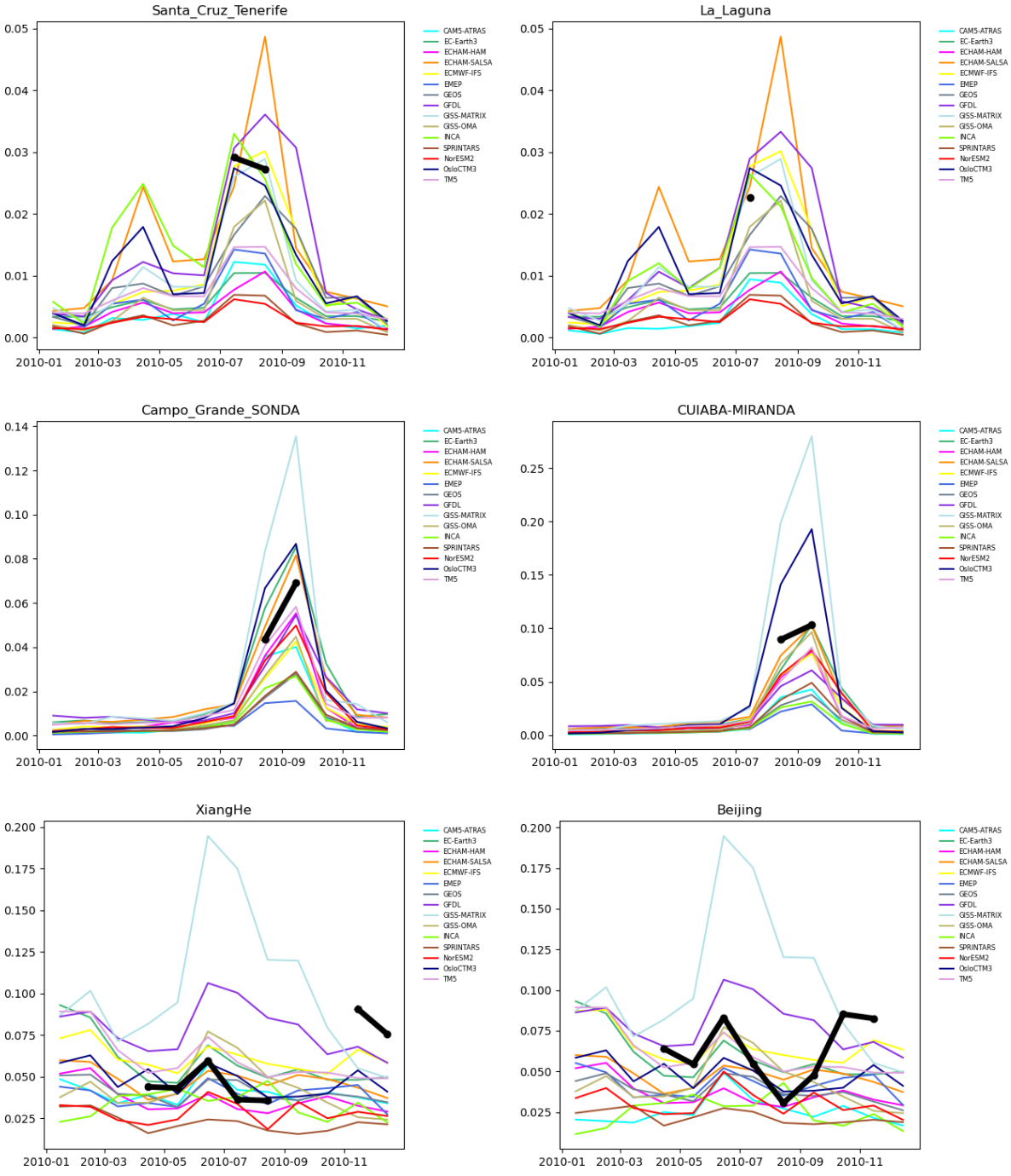

Fig S2: Seasonal cycle in total AAOD at 6 AERONET stations, influenced by desert dust; Santa_Cruz_Tenerife (28.47N, 16.25W) and La_Laguna (28.48N, 16.32W), by biomass burning; Campo_Grande_SONDA (20.44S, 54.54W), CUIABA-MIRANDA (15.73S, 56.07W), and by industrial emissions; XiangHe (39.75N, 116.96E) and Beijing (39.98N, 116.38E).

20

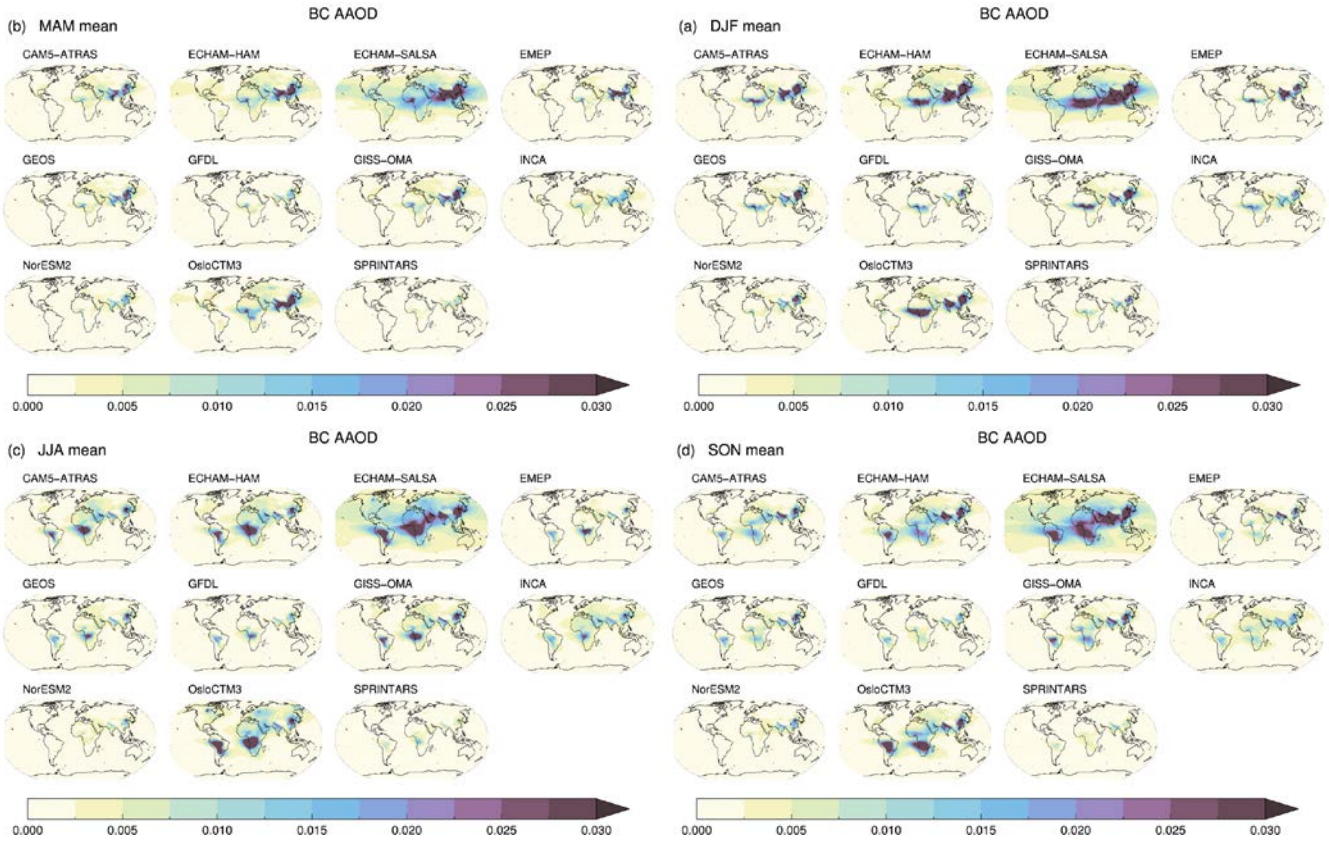

Figure S3: BC absorption at λ = 550 nm in AeroCom Phase III; (a) DJF mean, (b) MAM mean, (c) JJA mean and (d) SON mean

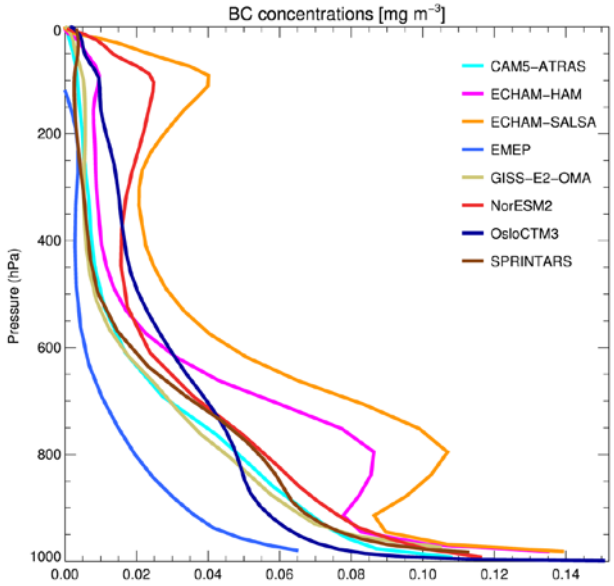

25

Figure S4: Global mean vertical distribution of BC concentrations [mg m-3] in AeroCom Phase III.

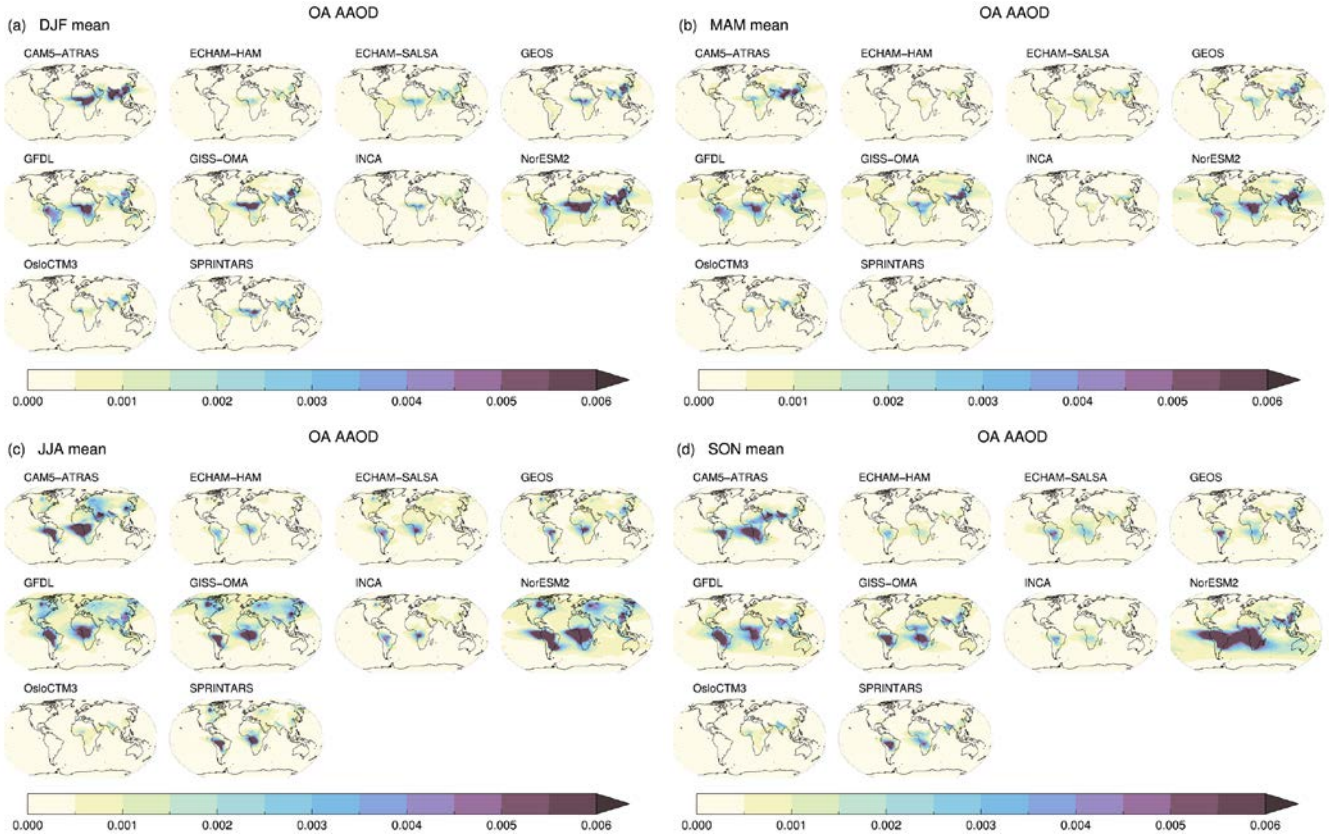

Figure S5: OA absorption at λ = 550 nm in AeroCom Phase III; (a) DJF mean, (b) MAM mean, (c) JJA mean and (d) SON mean

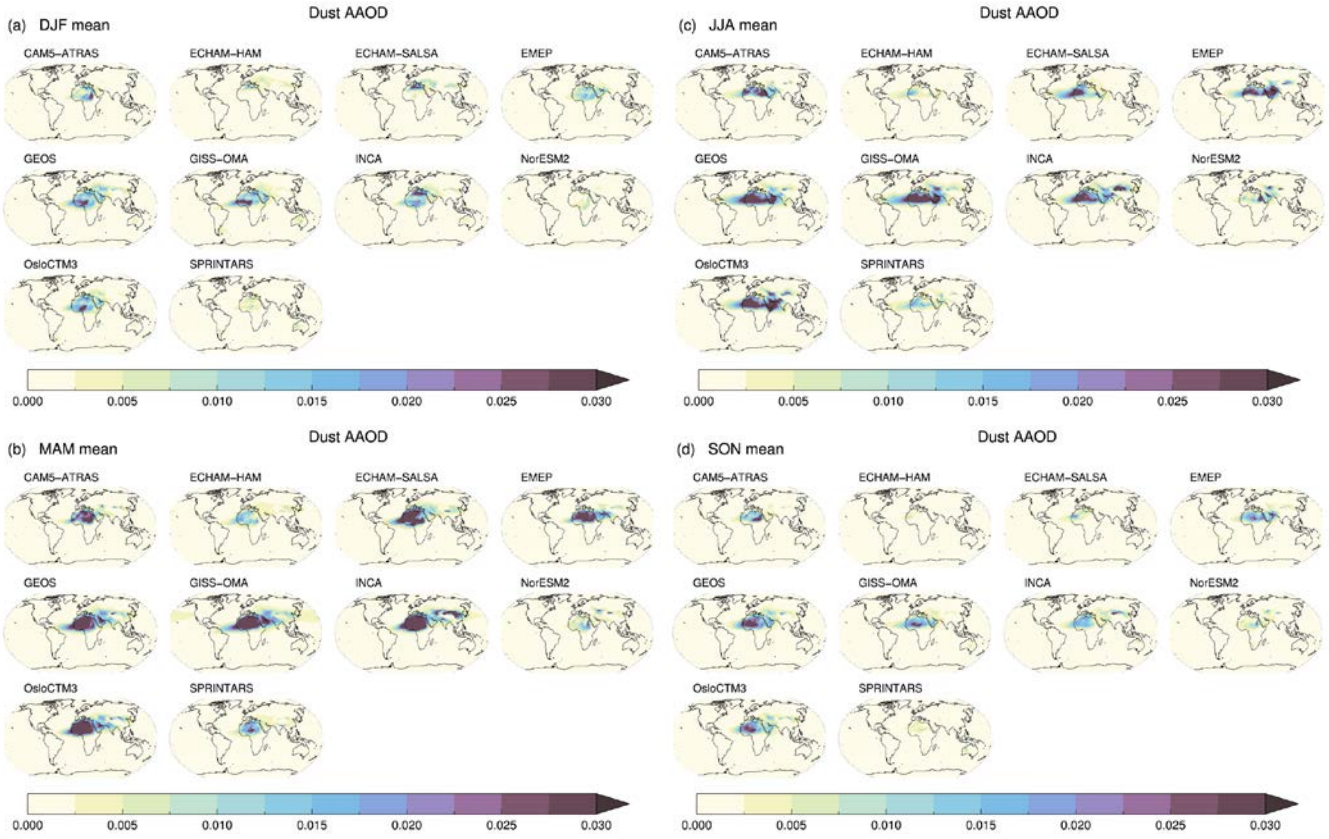

Figure S6: Dust absorption at λ = 550nm in AeroCom Phase III; (a) MAM mean, (b) SON mean

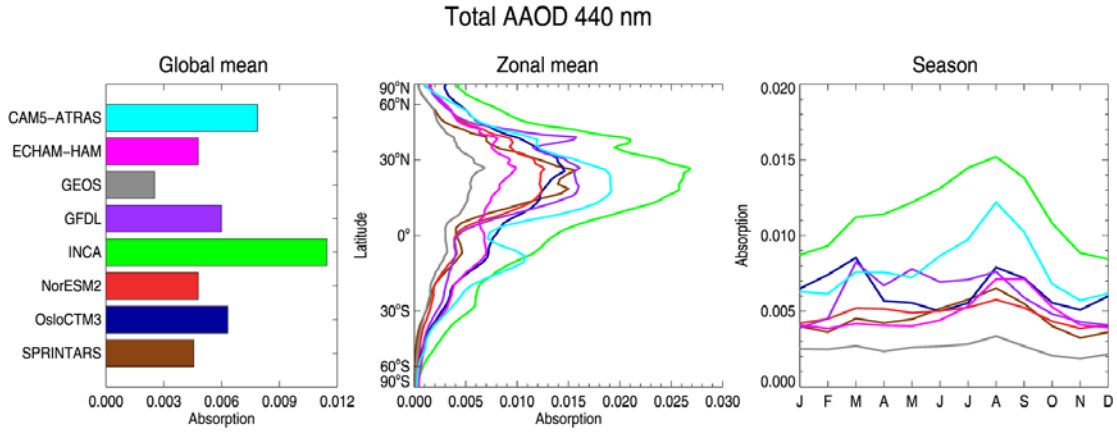

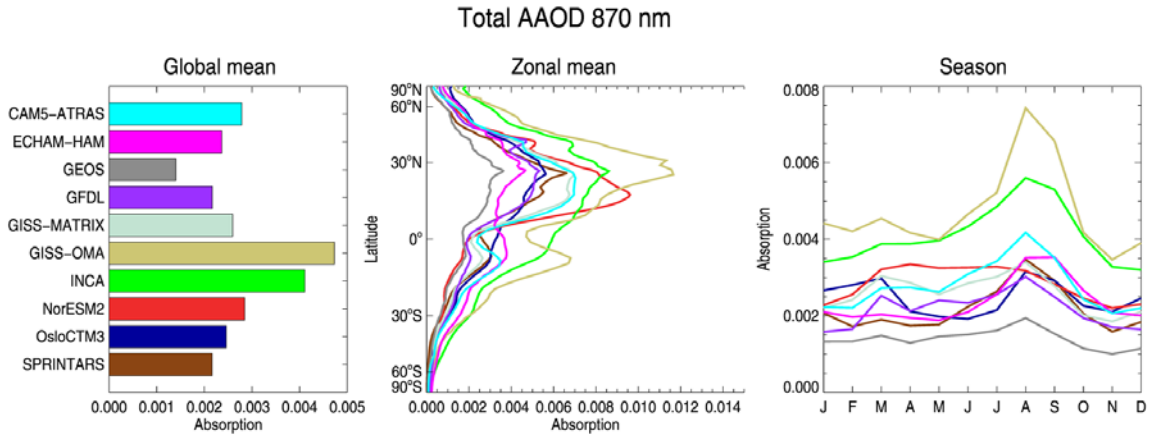

Figure S7: Total aerosol absorption at λ = 440nm and λ = 870nm; global mean, zonal mean and the seasonal cycle.

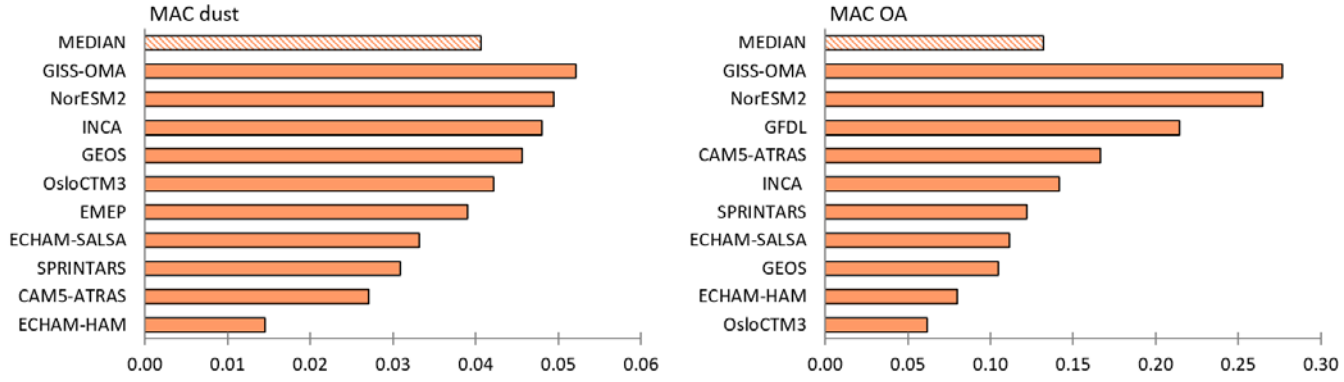

55

Figure S8: Global mean MAC values for each model for dust (left) and OA (right).

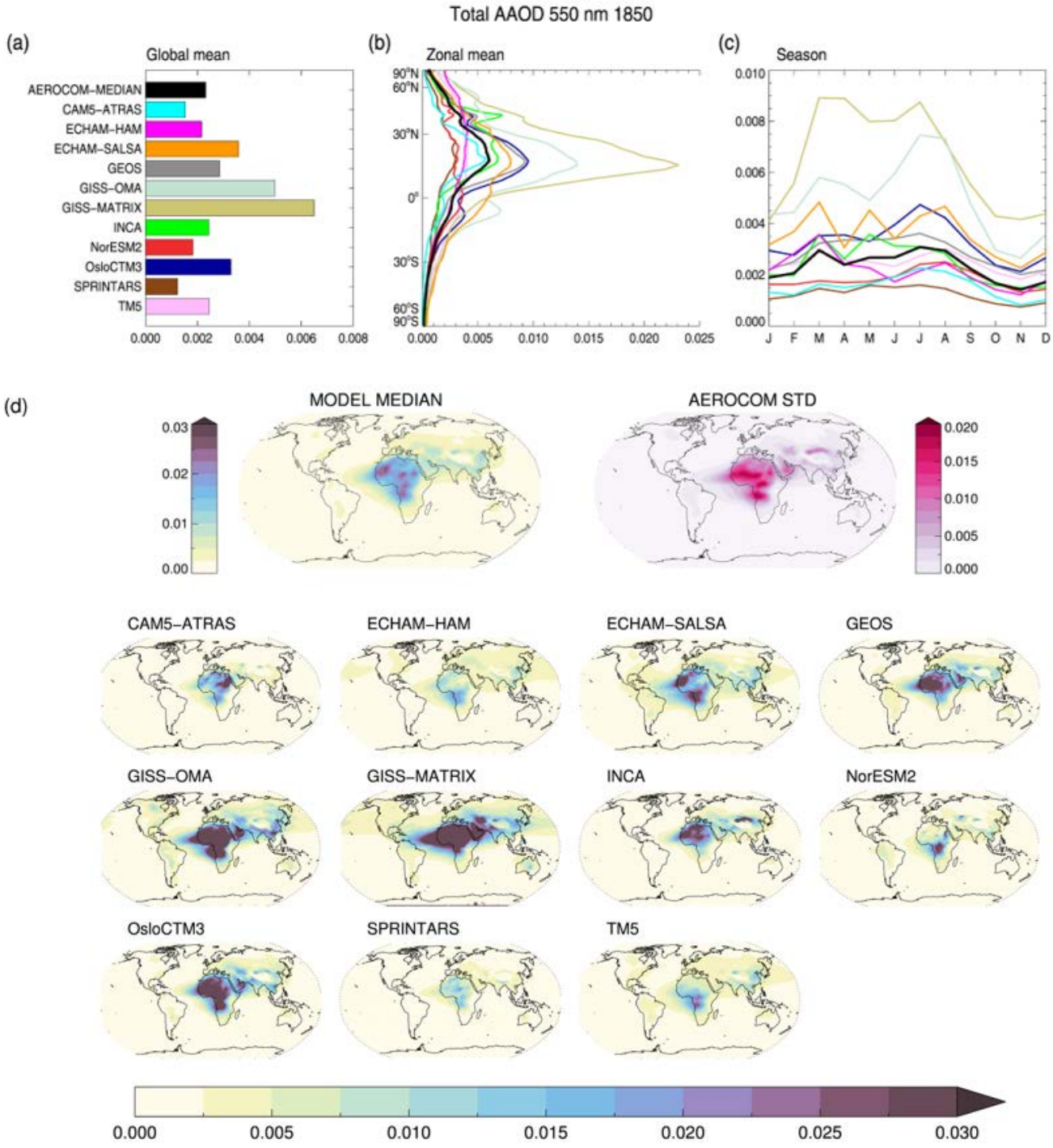

Figure S9: Total AAOD λ = 550 nm in 1850 from the models; (a) annual global mean, (b) annual zonal mean (c) the global seasonal cycle and (d) annual mean spatial distributions.

References

Bai, Z., Cui, X., Wang, X., Xie, H., and Chen, B.: Light absorption of black carbon is doubled at Mt. Tai and typical urban area in North China, Science of The Total Environment, 635, 1144-1151, https://doi.org/10.1016/j.scitotenv.2018.04.244, 2018.

Bond, T. C., and Bergstrom, R. W.: Light absorption by carbonaceous particles: An investigative review, Aerosol Science And Technology, 40, 27-67, 2006.

Budhavant, K., Andersson, A., Holmstrand, H., Bikkina, P., Bikkina, S., Satheesh, S. K., and Gustafsson, Ö.: Enhanced Light-Absorption of Black Carbon in Rainwater Compared With Aerosols Over the Northern Indian Ocean, J. Geophys. Res., 125, e2019JD031246, https://doi.org/10.1029/2019JD031246, 2020.

Cho, C., Kim, S.-W., Lee, M., Lim, S., Fang, W., Gustafsson, Ö., Andersson, A., Park, R. J., and Sheridan, P. J.: Observation-based estimates of the mass absorption cross-section of black and brown carbon and their contribution to aerosol light absorption in East Asia, Atmos. Environ., 212, 65-74, https://doi.org/10.1016/j.atmosenv.2019.05.024, 2019.

Cozic, J., Verheggen, B., Weingartner, E., Crosier, J., Bower, K. N., Flynn, M., Coe, H., Henning, S., Steinbacher, M., Henne, S., Collaud Coen, M., Petzold, A., and Baltensperger, U.: Chemical composition of free tropospheric aerosol for PM1 and coarse mode at the high alpine site Jungfraujoch, Atmos. Chem. Phys., 8, 407-423, 10.5194/acp-8-407-2008, 2008.

Cui, X., Wang, X., Yang, L., Chen, B., Chen, J., Andersson, A., and Gustafsson, Ö.: Radiative absorption enhancement from coatings on black carbon aerosols, Science of The Total Environment, 551–552, 51-56, http://dx.doi.org/10.1016/j.scitotenv.2016.02.026, 2016.

Doran, J. C., Barnard, J. C., Arnott, W. P., Cary, R., Coulter, R., Fast, J. D., Kassianov, E. I., Kleinman, L., Laulainen, N. S., Martin, T., Paredes-Miranda, G., Pekour, M. S., Shaw, W. J., Smith, D. F., Springston, S. R., and Yu, X. Y.: The T1-T2 study: evolution of aerosol properties downwind of Mexico City, Atmos. Chem. Phys., 7, 1585-1598, 10.5194/acp-7-1585-2007, 2007.

Forello, A. C., Bernardoni, V., Calzolai, G., Lucarelli, F., Massabò, D., Nava, S., Pileci, R. E., Prati, P., Valentini, S., Valli, G., and Vecchi, R.: Exploiting multi-wavelength aerosol absorption coefficients in a multi-time resolution source apportionment study to retrieve source-dependent absorption parameters, Atmos. Chem. Phys., 19, 11235-11252, 10.5194/acp-19-11235-2019, 2019.

Hitzenberger, R., Petzold, A., Bauer, H., Ctyroky, P., Pouresmaeil, P., Laskus, L., and Puxbaum, H.: Intercomparison of Thermal and Optical Measurement Methods for Elemental Carbon and Black Carbon at an Urban Location, Environmental Science & Technology, 40, 6377-6383, 10.1021/es051228v, 2006.

Knox, A., Evans, G. J., Brook, J. R., Yao, X., Jeong, C. H., Godri, K. J., Sabaliauskas, K., and Slowik, J. G.: Mass Absorption Cross-Section of Ambient Black Carbon Aerosol in Relation to Chemical Age, Aerosol Science and Technology, 43, 522-532, 10.1080/02786820902777207, 2009.

Laborde, M., Crippa, M., Tritscher, T., Jurányi, Z., Decarlo, P. F., Temime-Roussel, B., Marchand, N., Eckhardt, S., Stohl, A., Baltensperger, U., Prévôt, A. S. H., Weingartner, E., and Gysel, M.: Black carbon physical properties and mixing state in the European megacity Paris, Atmos. Chem. Phys., 13, 5831-5856, 10.5194/acp-13-5831-2013, 2013.

Lan, Z.-J., Huang, X.-F., Yu, K.-Y., Sun, T.-L., Zeng, L.-W., and Hu, M.: Light absorption of black carbon aerosol and its enhancement by mixing state in an urban atmosphere in South China, Atmos. Environ., 69, 118-123, https://doi.org/10.1016/j.atmosenv.2012.12.009, 2013.

Levy, M. E., Zhang, R., Khalizov, A. F., Zheng, J., Collins, D. R., Glen, C. R., Wang, Y., Yu, X.-Y., Luke, W., Jayne, J. T., and Olaguer, E.: Measurements of submicron aerosols in Houston, Texas during the 2009 SHARP field campaign, J. Geophys. Res. - Atmos., 118, 10,518-510,534, 10.1002/jgrd.50785, 2013.

Ma, Y., Huang, C., Jabbour, H., Zheng, Z., Wang, Y., Jiang, Y., Zhu, W., Ge, X., Collier, S., and Zheng, J.: Mixing state and light absorption enhancement of black carbon aerosols in summertime Nanjing, China, Atmos. Environ., 222, 117141, https://doi.org/10.1016/j.atmosenv.2019.117141, 2020.

Myhre, G., Samset, B. H., Schulz, M., Balkanski, Y., Bauer, S., Berntsen, T. K., Bian, H., Bellouin, N., Chin, M., Diehl, T., Easter, R. C., Feichter, J., Ghan, S. J., Hauglustaine, D., Iversen, T., Kinne, S., Kirkevåg, A., Lamarque, J. F., Lin, G., Liu, X., Lund, M. T., Luo, G., Ma, X., van Noije, T., Penner, J. E., Rasch, P. J., Ruiz, A., Seland, Ø., Skeie, R. B., Stier, P., Takemura, T., Tsigaridis, K., Wang, P., Wang, Z., Xu, L., Yu, H., Yu, F., Yoon, J. H., Zhang, K., Zhang, H., and Zhou, C.: Radiative forcing of the direct aerosol effect from AeroCom Phase II simulations, Atmos. Chem. Phys., 13, 1853-1877, 10.5194/acp-13-1853-2013, 2013.

Pandolfi, M., Ripoll, A., Querol, X., and Alastuey, A.: Climatology of aerosol optical properties and black carbon mass absorption cross section at a remote high-altitude site in the western Mediterranean Basin, Atmos. Chem. Phys., 14, 6443-6460, 10.5194/acp-14-6443-2014, 2014.

Presler-Jur, P., Doraiswamy, P., Hammond, O., and Rice, J.: An evaluation of mass absorption cross-section for optical carbon analysis on Teflon filter media, Journal of the Air & Waste Management Association, 67, 1213-1228, 10.1080/10962247.2017.1310148, 2017.

Ram, K., and Sarin, M. M.: Absorption Coefficient and Site-Specific Mass Absorption Efficiency of Elemental Carbon in Aerosols over Urban, Rural, and High-Altitude Sites in India, Environmental Science & Technology, 43, 8233-8239, 10.1021/es9011542, 2009.

Reche, C., Querol, X., Alastuey, A., Viana, M., Pey, J., Moreno, T., Rodríguez, S., González, Y., Fernández-Camacho, R., de la Rosa, J., Dall'Osto, M., Prévôt, A. S. H., Hueglin, C., Harrison, R. M., and Quincey, P.: New considerations for PM, Black Carbon and particle number concentration for air quality monitoring across different European cities, Atmos. Chem. Phys., 11, 6207-6227, 10.5194/acp-11-6207-2011, 2011.

Subramanian, R., Kok, G. L., Baumgardner, D., Clarke, A., Shinozuka, Y., Campos, T. L., Heizer, C. G., Stephens, B. B., de Foy, B., Voss, P. B., and Zaveri, R. A.: Black carbon over Mexico: the effect of atmospheric transport on mixing state, mass absorption cross-section, and BC/CO ratios, Atmos. Chem. Phys., 10, 219-237, 10.5194/acp-10-219-2010, 2010.

Wang, Q., Jacob, D. J., Spackman, J. R., Perring, A. E., Schwarz, J. P., Moteki, N., Marais, E. A., Ge, C., Wang, J., and Barrett, S. R. H.: Global budget and radiative forcing of black carbon aerosol: Constraints from pole-to-pole (HIPPO) observations across the Pacific, J. Geophys. Res., 119, 195-206, https://doi.org/10.1002/2013JD020824, 2014.

Wang, Q., Huang, R., Zhao, Z., Cao, J., Ni, H., Tie, X., Zhu, C., Shen, Z., Wang, M., Dai, W., Han, Y., Zhang, N., and Prévôt, A. S. H.: Effects of photochemical oxidation on the mixing state and light absorption of black carbon in the urban atmosphere of China, Environ. Res. Lett., 12, 044012, 10.1088/1748-9326/aa64ea, 2017.

Weyant, C. L., Shepson, P. B., Subramanian, R., Cambaliza, M. O. L., Heimburger, A., McCabe, D., Baum, E., Stirm, B. H., and Bond, T. C.: Black Carbon Emissions from Associated Natural Gas Flaring, Environmental Science & Technology, 50, 2075-2081, 10.1021/acs.est.5b04712, 2016.

You, R., Radney, J. G., Zachariah, M. R., and Zangmeister, C. D.: Measured Wavelength-Dependent Absorption Enhancement of Internally Mixed Black Carbon with Absorbing and Nonabsorbing Materials, Environmental Science & Technology, 50, 7982-7990, 10.1021/acs.est.6b01473, 2016.

Yttri, K. E., Lund Myhre, C., Eckhardt, S., Fiebig, M., Dye, C., Hirdman, D., Ström, J., Klimont, Z., and Stohl, A.: Quantifying black carbon from biomass burning by means of levoglucosan – a one-year time series at the Arctic observatory Zeppelin, Atmos. Chem. Phys., 14, 6427-6442, 10.5194/acp-14-6427-2014, 2014.

Zanatta, M., Gysel, M., Bukowiecki, N., Müller, T., Weingartner, E., Areskoug, H., Fiebig, M., Yttri, K. E., Mihalopoulos, N., Kouvarakis, G., Beddows, D., Harrison, R. M., Cavalli, F., Putaud, J. P., Spindler, G., Wiedensohler, A., Alastuey, A., Pandolfi, M., Sellegri, K., Swietlicki, E., Jaffrezo, J. L., Baltensperger, U., and Laj, P.: A European aerosol phenomenology-5: Climatology of black carbon optical properties at 9 regional background sites across Europe, Atmos. Environ., 145, 346-364, https://doi.org/10.1016/j.atmosenv.2016.09.035, 2016.

Zhang, Q., Shen, Z., Lei, Y., Zhang, T., Zeng, Y., Ning, Z., Sun, J., Westerdahl, D., Xu, H., Wang, Q., Cao, J., and Zhang, R.: Optical properties and source identification of black carbon and brown carbon: comparison of winter and summer haze episodes in Xi'an, Northwest China, Environmental Science: Processes & Impacts, 21, 2058-2069, 10.1039/C9EM00320G, 2019.